Density of states of a two-dimensional electron gas at semiconductor surfaces

Maria Grazia Betti

Istituto Nazionale per la Fisica della Materia, Dipartimento di Fisica, Università di Roma ''La Sapienza,''
Piazzale Aldo Moro 2, I-00185 Roma, Italy

V. Corradini, G. Bertoni, P. Casarini, and Carlo Mariani

Istituto Nazionale per la Fisica della Materia, Dipartimento di Fisica, Università di Modena e Reggio Emilia,
Via G. Campi 213/A, I-41100 Modena, Italy

A. Abramo

DEGM, Università di Udine, Via delle Scienze 208, I-33100 Udine, Italy

The formation of a two-dimensional (2D) electron channel at semiconductor surfaces has been studied by high-luminosity and high energy-resolution ultraviolet photoelectron spectroscopy. A large variety of band-bending sources (alkali metals, silver and antimony adatoms, cleavage defects) on different narrow-gap III-V(110) substrates (InAs, InSb) has been used. The measured photoemission spectral density in the semiconductor conduction band shows a steplike structure, consistent with the description of a jelliumlike 2D electron gas confined in a potential well, and it is independent of the band-bending sources. A self-consistent solution of the Poisson and Schrödinger equations gives the energy eigenvalues, the eigenstates, and the spectral density, in excellent agreement with the collection of photoemission results. Moreover, the accumulated charge density ranges between 3×10^{11} and 2×10^{12} electrons/cm^2, consistent with previous experimental results on plasmon excitations.

I. INTRODUCTION

In semiconductor devices, two-dimensional (2D) electron channels are created at heterostructures or metal-oxide-semiconductors (MOS's), where carriers are confined to the vicinity of junction between layers of semiconductors.[1] In 1957, Schrieffer first postulated that the electron confinement in narrow potential wells of an inversion layer should result in a nonclassical behavior.[2] The electrons or holes are constrained in one dimension and they can occupy quantized energy levels if the spatial dimension of the channel is comparable to the carrier wavelength. At a free semiconductor surface a degenerate 2D electron gas can be created accumulating electronic charge deriving from a low density of defects or metal adatoms deposited at the surface.

After the first direct observation of a surface-bound state of electrons localized in a narrow accumulation layer at the InAs-oxide interface in a pioneering work by Tsui,[3] the Landau-level structure of the 2D energy bands and the optical and transport properties of narrow accumulation and inversion layers were studied by several authors.[1] Although Schottky-barrier formation at metal-semiconductor interfaces has been an active subject of research in semiconductor physics, only few works have been devoted to the electronic properties of the 2D electron channel at well-characterized semiconductor surfaces. Collective excitations in confined 2D electron gases at semiconductor surfaces, i.e., plasma modes, have been considered by several authors,[4–8] but an exhaustive experimental study of the spectral density evolution as a function of the band-bending potential is still lacking.

We present an investigation of the spectral density at the discrete quantized electronic levels populated in the conduction band of narrow gap III-V(110) surfaces (InAs and InSb) after deposition of different metals (alkali, silver, antimony) or producing cleavage defects, by means of high energy-resolution and high-luminosity UV photoemission spectroscopy.

Photoelectron spectroscopy is the most direct method for a detailed characterization of the occupied electronic states, but it requires high sensitivity and luminosity to detect low spectral density of states (below 10^{12} electrons/cm^2). A photoemission study of clean InAs surfaces prepared by either ion bombardment and annealing or by molecular-beam epitaxy (MBE) has reported an emission from the conduction band due to the charge accumulated in the near-surface region.[9] The authors indicate that the asymmetric line shape of the spectral density can be attributed to the presence of two discrete quantum levels, though they were not clearly resolved. The origin of the measured density of states was still controversial: defect-induced states in the semiconductor gap or charge accumulation in the conduction band? Aristov *et al.*[10,11] have performed a photoemission experiment where a giant accumulation layer was induced by depositing Cs on the InAs(110) surface. A spectral density of electronic states from the conduction-band levels localized at the $\bar{\Gamma}$ point of the Brillouin zone has been measured only for the maximum band bending achieved. They proposed a theoretical model to explain the energy levels confined within the potential well, obtaining only a qualitative agreement. Recently, we have presented preliminary photoemission results on the Cs/InAs(110) interface as a function of Cs coverage for different potential wells.[12] The discrete steplike density of states can

be univocally attributed to the 2D electron gas confined at the semiconductor surface.

Questions are still open: Is the accumulation channel at a semiconductor surface well described by a jelliumlike 2D electron gas confined in a potential well, and is it independent of the band-bending source? Is it only determined by the macroscopic substrate band parameters? To answer to these questions we examine and present herewith a wide class of physical systems with different band-bending sources, different atomic geometry of the adlayers, and different substrates and temperatures. An important requisite is to avoid metal systems where interdiffusion and reactivity preclude a univocal description of the physical process. Alkali metals and antimony deposited on the III-V(110) surfaces are unreactive and noninterdiffusing interfaces, model systems for the study of Schottky-barrier formation. Though silver presents a slight interdiffusion even at low temperature,[13] it is a good candidate for comparison with the previous model systems.

The electrons photoemitted from the conduction band of the InAs(110) and InSb(110) surfaces show a steplike spectral density when the band-bending source is due to either metal adatoms, or disorder-induced levels, or cleavage defects. The intensity and the width of the spectral density are independent of the band-bending sources and they are univocally determined only by the bulk doping and the depth of the potential profile. The spectral density and the energy eigenvalue set for a 2D electron gas can be related to the macroscopic properties, like the band-bending potential and space charge through comparison with a self-consistent calculation of the Poisson and Schrödinger equations. Their solutions give the potential well shape, the subband energy levels, and the accumulated charge density for the 2D electron gas, in excellent agreement with the whole set of experimental results. The charge density can be compared with the plasmon excitations energy deduced from high-resolution electron-energy-loss spectroscopy.

The paper is organized as follows: after an experimental section (Sec. II), Sec. III collects spectral density measurements of Cs, K, Ag, and Sb deposited on InAs(110) and Cs on InSb(110), Sec. IV is devoted to a theoretical description of the 2D electron gas at semiconductor surface, via a self-consistent solution of the Poisson-Schrödinger equations, enlightening the relationship between microscopic properties (eigenfunctions, energy eigenvalues) and macroscopic phenomena (charge density, band-bending potential profile). The conclusions are outlined in Sec. V.

II. EXPERIMENTAL DETAILS

The experiments, carried out at the surface physics laboratory LOTUS, were performed in ultrahigh vacuum (UHV) chambers containing a high-resolution ultraviolet photoelectron spectroscopy (HRUPS) apparatus and other ancillary facilities for sample preparation.

All photoelectron spectra reported here were excited with a high-intensity He discharge lamp (He I$_\alpha$ and He II$_\alpha$ photons, $h\nu = 21.218$ and 40.814 eV, respectively). The photoemitted electrons were analyzed in the plane of incidence,

with a high-resolution Scienta SES-200 hemispherical analyzer, with an integration angle of about $\pm 8°$ with respect to the normal emission direction. A good compromise among the signal-to-noise ratio, good energy resolution, and acquisition time (in order to avoid contamination) was obtained using 10-eV pass energy and 0.8-mm slits. In these conditions the energy resolution was better than 25 meV, as determined on the Fermi level (E_F) of freshly evaporated Au in good electrical contact with the semiconductor single crystals.

The InAs and InSb single crystals were *n*-type doped bars ($n = 4.5 \times 10^{17}$ atoms/cm^3 and $n = 8 \times 10^{15}$ atoms/cm^3, respectively). The (110) clean surfaces were obtained by cleaving *in situ*. Alkali metals were evaporated from well out gassed SAES Getters alkali dispensers at a pressure better than 7×10^{-11} mbar on the semiconductor substrates at different temperatures. Antimony was sublimated from Sb shots contained in a resistively heated quartz pipe. Silver was evaporated from a wire contained in a tungsten crucible. The evaporation rates were kept at about 0.1 monolayer (ML)/min. The adlayer thickness was determined by a crystal thickness monitor for Ag and Sb, while the Cs coverage calibration was checked by the evolution of the Cs $5p$ core-level intensity and work-function change, as a function of deposition time. One monolayer is defined as Sb or Ag atomic densities equivalent to the surface atomic density of InAs(110) (7.76×10^{14} atoms/cm^2), and it corresponds to nominal laminar coverage of 2.35 Å for Sb and 1.32 Å for Ag, respectively. The saturation coverage $\Theta = \Theta_S$ of Cs deposited on InAs(110) and InSb(110) is defined in Ref. 14 from the scanning tunneling microscopy images and it corresponds to the saturation value for the Cs $5p$ core-level intensities.

III. SPECTRAL DENSITY OF STATES IN THE CONDUCTION BAND OF SEMICONDUCTOR SURFACES

A selected set of energy distribution curves (EDC's) of the clean InAs(110) and InSb(110) surfaces and after a tiny deposition of alkali metal, covering the energy region of the upper valence band and the lowest conduction band, is shown in Fig. 1. At the very first metal deposition, the valence band is rigidly shifted towards higher binding energy without any significant modification of its structures, while a slight intensity decrease of the III-V related surface features occurs at higher alkali coverage. A low spectral density of states (about $\frac{1}{100}$ of the emission from the valence band) with a steplike line shape can be clearly observed within the conduction band, rising as a function of coverage in the very first deposition phase. Along with the increasing intensity of the spectral density of states in the III-V(110) conduction band, a downward band bending is measured from the In $4d$ core-level shift, as shown in Fig. 2. At extremely low alkali-metal coverage, the Fermi level pins well into the conduction band, the downward band bending presents a maximum accumulation [$V_{bb} = 520$ meV at $0.07\Theta_s$ of K/InAs(110) and $V_{bb} = 292$ meV at $0.01\Theta_s$ of Cs/InSb(110)], followed by a decrease for further alkali-metal deposition. This maximum value of the downward band bending occurs at the same
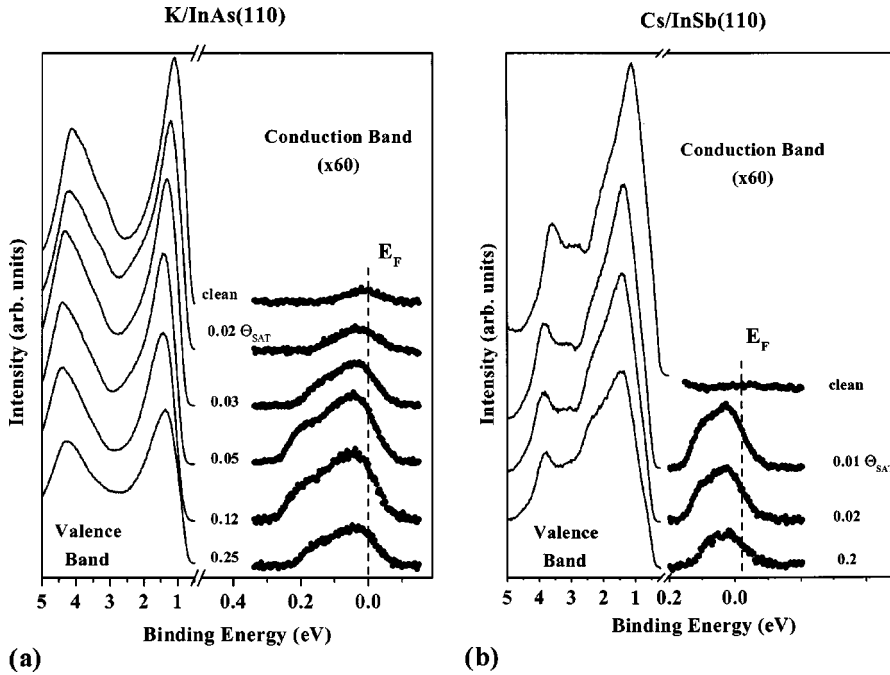
FIG. 1. Angle-integrated HRUPS spectra in the valence-band and conduction-band energy region for (a) the clean n-type doped InAs(110) surface and the K/InAs(110) interface at different K coverages; (b) the clean n-type doped InSb(110) surface and the Cs/InSb(110) interface at different Cs coverages. The energy scale for the conduction-band spectra is magnified by a factor of 10. The vertical bar marks the Fermi energy position. Photon energy of 21.218 eV (H I$_\alpha$).

alkali-metal coverage for which the highest density of states is emitted from the conduction band. Thus, the steplike spectral density can be related to the formation of discrete levels within the potential well induced by the downward pinned band at the surface, as already observed in previous papers for the Cs/InAs(110) interface.[11,12] A slight emission from the conduction band is present at the clean InAs(110) surface, while it not detectable at InSb(110). As it will be discussed in the following section, it relies on the doping-level-dependent Fermi-level position with respect to the conduction-band (CB) minimum for the substrate with different doping levels, thus it is positioned well into the CB for InAs and within the energy gap for InSb.

The coexistence of an unoccupied III-V(110) surface state populated when the small amount of alkali metal pushes the Fermi level in the conduction band can be hypothesized as well. Unoccupied surface states have been detected by photoemission spectroscopy after an artificial population of the surface band via optical pumping[15] or alkali-metal adsorption on the Ge(111) surface.[16] However, theoretical band-structure calculations for clean InAs(110) and InSb(110) predict an anion-related empty state far from the conduction-band minimum at the $\bar{\Gamma}$ point of surface Brillouin zone.[17] Also combined direct and inverse photoemission measurements[18] determine a surface gap in Γ of 1.7 eV [1.4 eV] for InAs(110) [InSb(110)], thus with the empty surface states positioned well into the conduction band. The absence of a Cs-induced state below $0.1\Theta_s$ of Cs has also been demonstrated by an angle-resolved photoemission experiment by Aristov *et al.*,[11] who measured a conduction-band emission localized at the $\bar{\Gamma}$ point. Therefore, we can reasonably rule out the occupation of a surface or alkali-metal-induced state as the origin of the observed spectral density in the CB.

Photoemission energy distribution curves from small alkali-metal deposition and for silver and antimony deposition on InAs(110) are shown as 3D plots in Fig. 3. The

perspective view focuses the attention on the energy gap region (light blue ''river''), bringing into evidence the relation between band bending formation and the evolution of the spectral density. On the left side (high binding energy) of the energy-gap region, the valence-band edge shifts to higher binding energy up to $0.07\Theta_s$ for K/InAs(110), as can be clearly deduced also from the top view projection [Fig. 3(a)]. No metal-induced structures are detectable in the whole band-gap region, up to the saturation coverage. The density of states in the conduction band emerges and it reaches the top of the *hill* in correspondence with the maximum band bending. Close to the saturation coverage, the K/InAs(110) interface presents a tail of induced states close to the valence-band maximum (VBM), while the spectral density in the CB decreases. A similar behavior has been already observed for Cs/InAs(110) and Cs/InSb(110).[12,19] The intensity decreasing of the emission from the conduction band at saturation coverage and the maximum emission achieved in correspondence with the maximum band bending are consistent with the band-bending-driven population of the InAs conduction band.

The analogous high-resolution photoemission experiment with silver [Fig. 3(b)] was performed on the InAs(110) substrate at 80 K to minimize interdiffusion processes. When as low as 0.01 ML of Ag is deposited, a finite density of states in the InAs conduction band appears. Also for this metal/semiconductor interface, the maximum band bending is reached in correspondence to the formation of the 2D electron channel in the bottom of the conduction band [see the projection on top of Fig. 3(b)]. The saturation value of the band-bending potential for the accumulation layer is $V_{bb} = 524$ meV at 0.01 ML of Ag, as determined from the In $4d$ core-level shift shown in Fig. 2. Although the metal source of band bending is different, the evolution of the spectral density of the conduction band for low metal coverage reflects the formation of the 2D electron gas confined at the
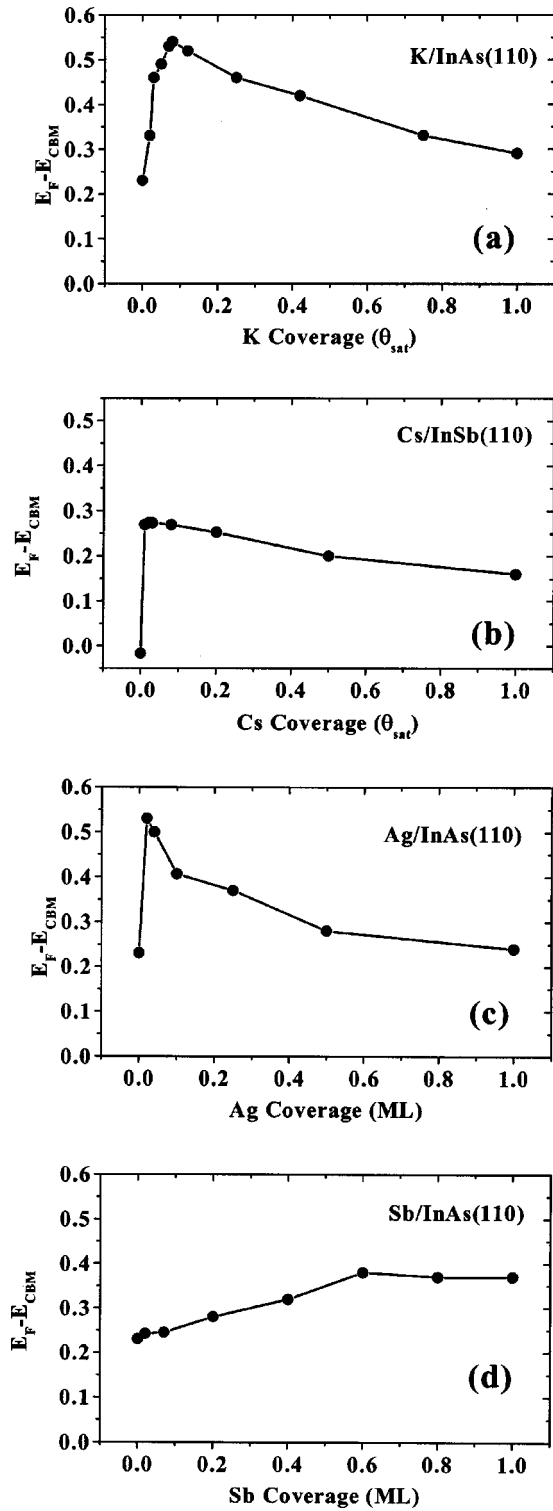
FIG. 2. Experimentally determined Fermi-level pinning (band-bending potential) as a function of metal exposure for different metal/III-V(110) systems. (a) K/InAs(110), (b) Cs/InSb(110), (c) Ag/InAs(110), (d) Sb/InAs(110). The continuous line through the data points is an eye guideline.
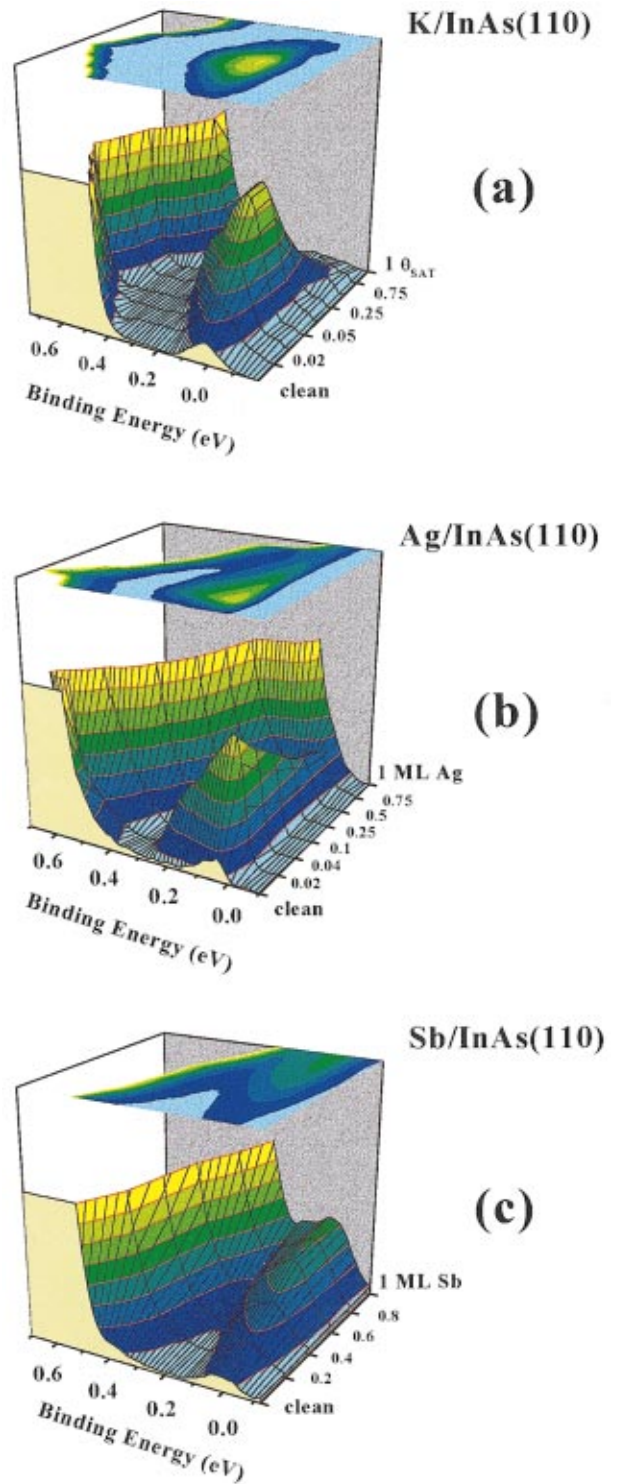

FIG. 3. (Color) Perspective 3D view of HRUPS spectra for the (a) K/InAs(110) (b) Ag/InAs(110), and (c) Sb/InAs(110) systems. The EDC intensity is displayed in the vertical axes, the binding energy referred to the Fermi level is reported along one of the horizontal axes, and successive spectra related to progressive metal deposition are stacked along the other horizontal axes.

surface. Further silver exposures induce an opposite movement of the Fermi-level pinning, distinguished by an upward band bending analogous to the evolution observed for alkali-metal deposition. However, while the alkali-metal/III-V(110) interfaces remain semiconducting up to the saturation coverage, the metallic Ag islands induce a spectral density within the projected bulk gap. In fact, at higher silver deposition (above 0.5 ML) a tail of ''metal-induced gap states'' can be detected above the valence-band maximum towards the Fermi level, and the 2D electron channel is depleted. The metallic states act as a trap for the electron charge accumulated at the surface.

A 3D plot of the EDC of the InAs(110) clean surface and after the deposition of Sb is sketched in Fig. 3(c). The saturation value of the band bending potential for the accumulation layer is lower than the previous cases ($V_{bb} = 375$ meV at 0.6 ML of Sb), as determined from the In $4d$ core-level shift (Fig. 2). The band-bending potential does not suddenly increase, in contrast with what observed for Ag and alkali-metal deposition, but it reaches a plateau at the completion of the first Sb monolayer. In the same coverage range, a low density of states above the valence-band maximum and close to the Fermi level is detectable. At variance with the previous interfaces, we clearly observe the coexistence of the 2D electron channel in the conduction band and the formation of Sb-induced states in the energy-gap region.

Alkali metals deposited on semiconductor surfaces are model systems for Schottky barrier formation; the adatoms/defects can induce donor-type electronic states, responsible for a long-range potential and charge accumulation at the surface. In narrow-gap n-type doped III-V semiconductors, alkali-metal donor-type states fix the Fermi level within the conduction band as already observed by several authors,[10–12] in contrast with the values expected from the MIGS theory.[20,21] At higher alkali-metal coverage, alkali-metal-induced states develop close to the valence-band maximum and are defined over all the surface Brillouin zone,[19] acting as a trap for the electronic charge accumulated at the surface. In these conditions, a depletion of the 2D electron gas channel has been observed. Antimony deposited on III-V(110) surfaces is a model system of an epitaxial continued layer structure.[22–24] The Sb adatoms continue the underlying substrate layer, forming large terraces without unbalancing the charge neutrality at the surface, at variance with alkali metals or Ag adatoms. However, at the edge of these terraces, Sb dangling bonds are present that can modify the local potential. A previous study of the Sb/GaAs(110) interface by scanning tunneling spectroscopy has detected gap states near the edge of Sb insulating terraces, arising from Sb dangling bonds.[25] They have been referred to as ''disorder-related'' features responsible of the Fermi-level pinning, inducing a maximum of charge accumulation with the completion of the ''quasiordered'' epitaxial layer. The formation of the 2D electron channel is determined by the presence of Sb-induced ''terrace edge'' states in the large Sb patches building up the quasiordered monolayer. The corresponding Sb interface states, well defined over all the surface Brillouin zone within the highly ordered epitaxial continued layer structure of the Sb large terraces, are present in the same

coverage range. This leads to a co-presence of the 2D electron channel in the conduction band and Sb occupied electronic states.

A band-bending potential can be also induced by the presence of defect states created in the surface preparation.[6,9] The intrinsic electron accumulation layer has been observed at reconstructed InAs(100) and InAs(111) surfaces grown by molecular beam epitaxy or prepared by ion bombardment and annealing (IBA).[9] A defect-induced accumulation or depletion layer has not been observed on well-cleaved (110) III-V surfaces, considered as an ideal prototype of defect-free surfaces. Given the n-type doping level of the crystals we have used, we expect the Fermi level to be positioned at 17 meV below the conduction-band minimum (CBM) for InSb, and at 88 meV above the CBM for InAs. Thus, we would expect a CB population of InAs even in the flat-band condition, as can be observed in Fig. 1(a). The photoelectron spectra previously reported for the clean cleaved surfaces present a slight emission in the conduction band only for InAs(110). A careful observation of the spectral density in the conduction band reveals an asymmetric density of states extended more than 150 meV below the Fermi level. The wider extension and the line shape of CB spectra density can be justified by the presence a 2D electron channel induced by cleavage defects, as will be theoretically justified in the next section.

Summarizing the experimental evidences collected and discussed above, the electrons photoemitted from the conduction band of the InAs(110) and InSb(110) surfaces show a steplike spectral density when the band-bending source is due to metal adatoms, disorder-induced levels, or cleavage defects. The intensity and the width of the spectral density are independent of the band-bending promoters but they seem univocally related to the bulk doping and to the depth of the potential profile. To confirm these hypotheses, in the following section we present a study of the density of states of a jelliumlike 2D electron gas confined at semiconductor surfaces, and a comparison to the whole set of the experimental results collected in different conditions.

IV. DENSITY OF STATES OF A 2D ELECTRON GAS AT A SEMICONDUCTOR SURFACE

A. Solution of the Poisson and Schrödinger equations for a 2D electron gas

The 2D electron gas formed at a semiconductor surface is confined along the z direction (perpendicular to the surface plane) and can be considered free in the xy plane. In the parabolic approximation, we expect a number of 2D electronic states per unit area $g_{2D}(E) = m_e^*/(\pi\hbar^2)\,\theta(E - E_0)$, where θ is the step function, m_e^* is the electron effective mass, and E_0 is the energy eigenvalue. The density of states is constant, independent of the energy and the layer thickness. If more subbands are present in the potential well, the spectral density will present additional steps in correspondence with the higher-energy eigenvalues E_n.[26]

We determine the eigenvalues, the eigenfunctions, the potential well, and the charge distribution via the self-
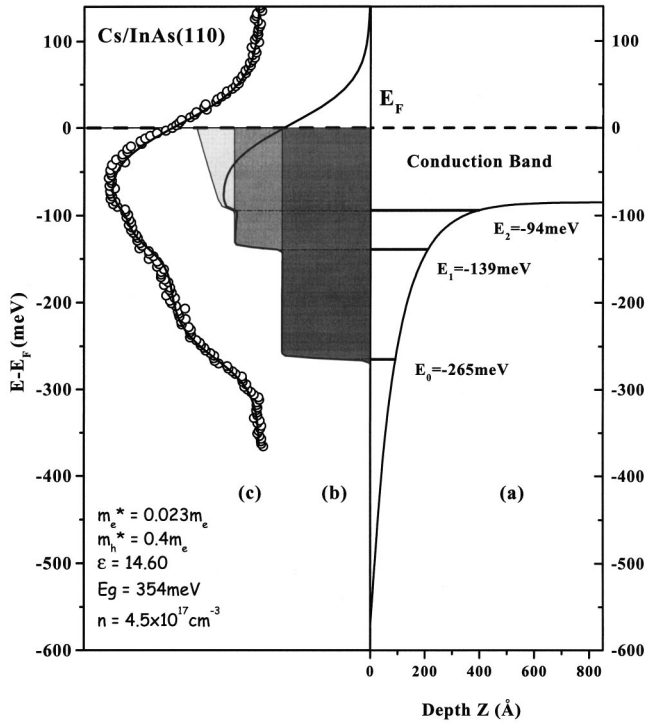
FIG. 4. Result of a self-consistent solution of the Poisson-Schrödinger equations for the Cs/InAs(110) system. (a) Potential well shape and subband energy levels in the subsurface region; (b) theoretical density of states in the parabolic approximation multiplied by the Fermi-Dirac distribution function at temperatures of 0 and 300 K; (c) photoemission experimental spectrum of the conduction band for $0.05\Theta_s$ Cs (white dots), and theoretical data calculated at room temperature (RT) and convoluted with the experimental broadening (continuous line).
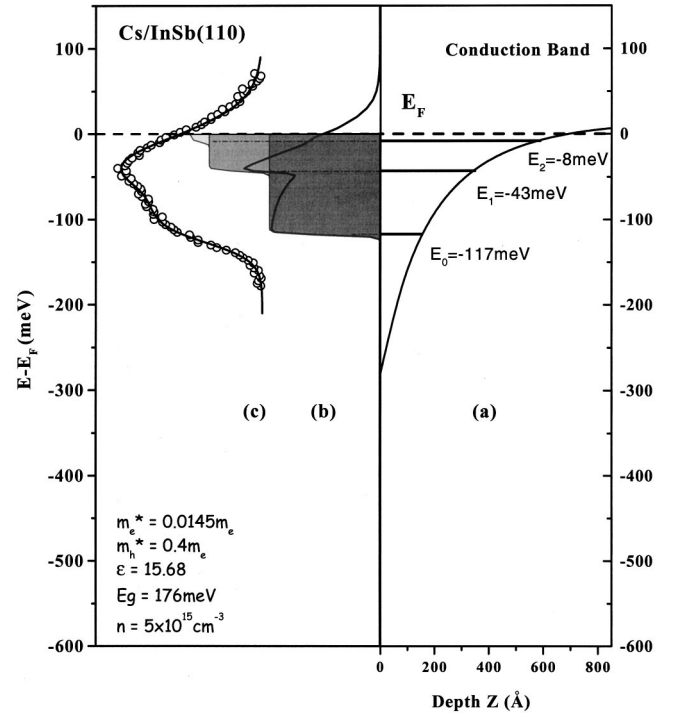
FIG. 5. Result of a self-consistent solution of the Poisson-Schrödinger equations for the Cs/InSb(110) system. (a) Potential well shape and subband energy levels in the subsurface region; (b) theoretical density of states in the parabolic approximation multiplied by the Fermi-Dirac distribution function at temperatures of 0 and 300 K; (c) photoemission experimental spectrum of the conduction band for $0.01\Theta_s$ Cs (white dots), and theoretical data calculated at RT and convoluted with the experimental broadening (continuous line).

consistent solution of the Poisson-Schrödinger system of equations. The Schrödinger and Poisson equations for a jelliumlike 2D electron gas are solved using an iterative Newton procedure. In the parabolic approximation, the Schrödinger equation is actually solved in the envelope-function approximation, where the crystal potential is considered in the parabolic approximation, and an external potential $V(z)$ (i.e., the band-bending potential) is superimposed. In addition, spherical symmetry is assumed for InAs (InSb), with parabolic mass of $m_e^* = 0.023m_e$ $(0.0145m_e)$ for the electrons and $m_h^* = 0.4m_e$ $(0.4m_e)$ for the holes, a dielectric constant of 14.60 (15.68) and the energy gap of 0.354 eV (0.176 eV) at room temperature (RT). The simulation starts by assuming an estimate for the electrostatic potential, as deduced by the experimental core-level measurements, and introducing the nominal doping concentration. The eigenvectors and energy eigenvalues are determined using the inverse iteration technique and Rayleigh quotient, respectively. Once the eigenstates are computed, the charge density for holes and for electrons are calculated, and then the nonlinear Poisson equation is solved using the Newton method. Since the quantum charge depends both on the eigenvalues (through density of states and Fermi statistics) and the eigenvectors (through the square modulus of the eigenfunctions), the Frechet derivative (i.e., Jacobian) of the system of equation is used.

The new potential profile obtained from the solution of Poisson equation is introduced to recompute the eigenstates and the procedure is iterated until the convergence is reached.

On the right panel (a) of Fig. 4 (Fig. 5) the potential well as a function of distance from the InAs (InSb) surface, and the first three quantized discrete energy levels, as obtained after the solution of the Poisson-Schrödinger equations, are displayed. The calculation is performed for the InAs (InSb) system with a potential well of 570 meV (280 meV) with respect to the Fermi level, corresponding to the experimentally measured band bending. The three lowest energy levels are at $E_0 = -264$ meV $[-117$ meV], $E_1 = -137$ meV $[-43$ meV], and $E_2 = -92$ meV $[-8$ meV] for the InAs(110) [InSb(110)] surface. The density of 2D electronic states $g_{2D}(E)$ multiplied by the Fermi-Dirac distribution function f_{FD} at 0 and 300 K is reported in the central panel (b) of Figs. 4 and 5, assuming the 2D spectral density constant for each eigenvalue E_n in the potential well, and simulating with a 3D free-electron gas the density of states from the bulk CBM to the Fermi level. This theoretical spectral density does not take into account the lifetime of the quasiparticle excitations. It is noteworthy that the experimental spectral density does not show a sharpening of the step onset upon lowering the temperature (80 K), and that the experimental step width is much larger than the energy resolution. Hence,
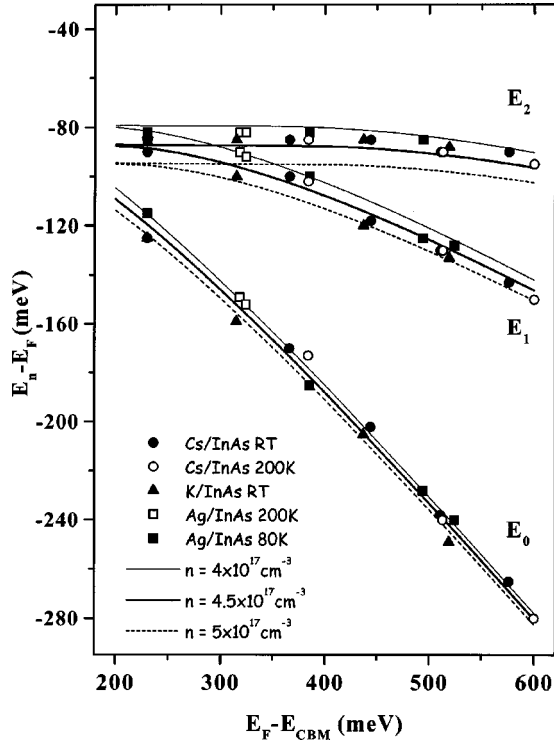
FIG. 6. Calculated and experimental energy eigenvalues for the InAs substrate, plotted as a function of the potential well depth ($E_F - E_{CBM}$), as deduced from the solution of Poisson-Schrödinger equations. The theoretical energy eigenvalues (lines) are calculated for InAs (parabolic mass of $0.023m_e$ for electrons and $0.4m_e$ for holes, dielectric constant of 14.60, energy gap of 0.354 eV at RT) at different values of doping level (ranging between 4×10^{17} and 5×10^{17} cm^{-3}). The bands thus obtained for each eigenvalue give an estimate of the doping-level-dependent theoretical uncertainty. The experimental energy eigenvalues (squares, circles and triangles), as deduced from the fitting procedure of the photoemission spectral density, are reported for a variety of systems. The corresponding energy values are also reported in Table I.

the onset width of each measured eigenvalue must depend on the finite excitation lifetime. We take into account this lifetime contribution[27] by convoluting the total density of states with a Lorentzian function. Moreover, we give a weight to the constant intensity of each subband, to take into account the experimental surface sensitivity and the z localization of the charge density for each eigenlevel (as will be discussed in Sec. IV B). The final theoretical results are plotted in Figs. 4(a) and 5(a) superimposed to the experimental data. The theoretical curves derived within these approximations are in excellent agreement with the experiments.

Within these hypothesis we can perform a fitting of the whole set of the experimental results discussed in Sec. II. The energy position of the discrete energy levels is obtained by fitting the experimental spectra with a steplike 2D electron density of states, multiplied by the Fermi-Dirac distribution function, and convoluted with a Gaussian representing the overall broadening. The theoretical eigenvalues obtained via the self-consistent solution of the Poisson-Schrödinger equations as a function of the potential bias, with respect to the conduction-band minimum (E_F

$-E_{CBM}$), are collected in Fig. 6 and reported in Table I, along with the results of the fitting procedure to the experimental data. The theoretical data are calculated within a range of doping level [$(4-5) \times 10^{17}$ cm^{-3}] to give an estimation of the theoretical uncertainty. The steplike density of states and the excellent theoretical agreement are obtained also on the clean cleaved InAs(110) surfaces, with a defect-induced band-bending potential of about 140 meV. This leads to an energy distance between the bottom of the surface conduction band and the Fermi level of about 230 meV. All the band-bending potential data collected in Table I are calculated summing this value to the band-bending potential deduced from the energy shift of the In $4d$ core level with respect to the clean cleaved surface. It is noteworthy to notice that the macroscopic input parameters are the same for the whole set of data in a wide range of band bending and substrate temperatures. These results confirm that a general model of a 2D jelliumlike electron gas well describes the charge accumulated at semiconductor surface and it is not dependent on the substrate, the atomic geometry of the adlayer, or the sources of band bending.

B. Charge density

In Fig. 7 we report the potential well and the energy eigenvalues for the InAs(110) and InSb(110) systems, calculated at the maximum band-bending experimentally achieved. For each eigenvalue we plot the charge density calculated through the square modulus of the eigenfunctions obtained from the solution of the Schrödinger equation. We observe that the potential well width along z is larger on InSb than on InAs, consistently with the lower doping of InSb, i.e., with the lower density of free carriers available to compensate the charge accumulation at the surface.

In a classical description, the charge density depends on the energy distance from the conduction-band minimum E_{CBM} to the Fermi level E_F, and it reaches the maximum value at the surface. In a quantum description, the free-electron density depends on the square modulus of the eigenfunction in the potential well, and the wave function $\phi_i(z)$ for each subband must have a node at the semiconductor surface ($z=0$). The boundary condition imposes zero charge at the surface; as a consequence the extension of the space charge region is wider in the quantum case than in the classical approximation. The first energy level E_0 presents its maximum of charge density at ~ 50 Å below the surface for InAs and at ~ 90 Å for InSb. As the quantum number increases, the charge-density distribution extends towards the bulk and its maximum is located even far from the surface. Given the experimental surface sensitivity, we preferentially access to the shallow electron density accumulated beneath the surface in the deepest energy levels. This explains the different weight adopted for each subband in the density of states reported in Figs. 4(a) and 5(a).

The number of electrons per unit area in each subband is

$$N_a = \int_{E_n}^{+\infty} g(E) f_{FD}(E) dE$$

$$= m_e^* / (\pi \hbar^2)((E_F - E_n)$$

$$+ kT \ln\{1 + \exp[(E_n - E_F)/kT]\}). \qquad (1)$$

TABLE I. Binding energy of the quantized eigenstates within the potential well, as deduced from the solution of the Poisson-Schrödinger equations (theory) calculated for the actual doping level ($n \sim 4.5 \times 10^{17} \, \text{cm}^{-3}$), compared with the results of a fitting procedure to the experimental data (Expt.). The quoted experimental errors are deduced from the fit procedure. This collection of energy eigenvalues is also plotted in Fig. 6.

Interface	$E_F - E_{CBM}$ (meV)	E_0		E_1		E_2	
		Theor. (meV)	Expt. (meV)	Theor. (meV)	Expt. (meV)	Theor. (meV)	Expt. (meV)
InAs clean	230	115	125 ± 10	81	90 ± 10	79	85 ± 10
Cs/InAs RT[a]	364	169	170 ± 5	97	100 ± 5	80	85
	442	204	202	110	118	81	85
	510	235	240	123	130	84	90
	568	263	262	135	143	88	90
Cs/InAs 200 K	384	178	173	100	102	80	85
	600	278	275	142	145	90	95
K/InAs RT	330	155	159 ± 5	92	100 ± 5	80	85
	460	212	205	113	120	82	85
	484	223	245	118	130	83	87
	519	239	249	125	133	85	88
Ag/InAs 80 K	385	178	185 ± 5	100	100 ± 5	80	83
	494	228	228	120	125	83	85
	524	242	240	126	128	85	85
Ag/InAs 200 K	318	150	149	90	90	80	82
	324	152	152	91	92	80	82

[a]RT denotes room temperature.

If the Fermi energy for the *n*-type semiconductor is above the CBM, as in the present case of InAs the total charge density includes also the contribution of the bulk dopant donors N_d. Thus, subtracting this last bulk contribution, we obtain the density of accumulated charge:

$$N_a = \int_{E_n}^{E_{CBM}} g(E) f_{FD}(E) dE$$

$$= m_e^* / (\pi \hbar^2)$$

$$\times \left[(E_{CBM} - E_n) + kT \ln \frac{1 + \exp[(E_n - E_F)/kT]}{1 + \exp[(E_{CBM} - E_F)/kT]} \right].$$

$$(2)$$

Following these hypotheses, we have calculated the total accumulated charge density for the maximum band bending achieved for all the experimental results, as reported in Table II for InAs. In the case of the clean cleaved surface, we observe an accumulated charge density of about 3×10^{11} electrons/cm^2 for InAs, due to the cleavage defects present at the surface. This induces a surface Fermi-level position of ~ 230 meV above the CBM for clean cleaved InAs, as reported in Table I. Previous work on MBE-grown surfaces estimated a density of accumulated charge ranging between 5×10^{11} and 10×10^{11} electrons/cm^2.[9] As far as it concerns the metal adatoms (Cs, K, Ag, Sb) the charge density accumulated in the subsurface region ranges from 7×10^{11} to 25×10^{11} electrons/cm^2. The charge accumulated at
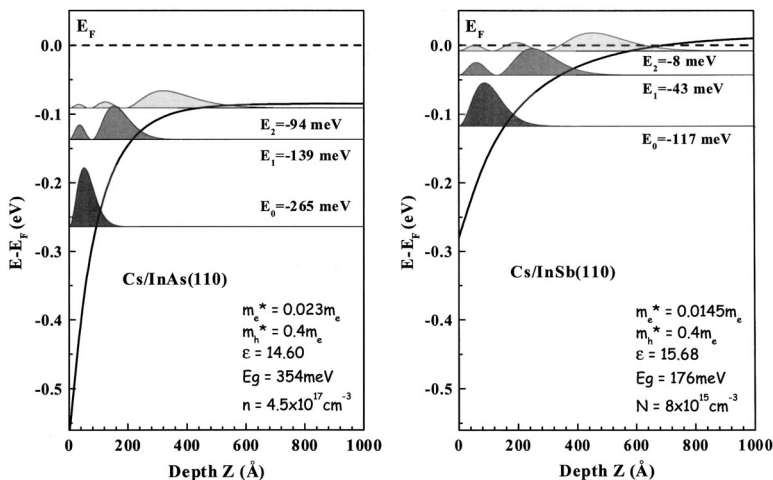

FIG. 7. Potential wells, subband energy levels, and the square modulus of the first three eigenfunctions for InAs(110) and InSb(110) (left and right panel, respectively), calculated at the maximum band bending achieved after the alkali-metal deposition, as a function of the distance from the surface (depth *z*). Note the same energy and depth scales in both panels to emphasize the physical dependence on the substrate parameters.

TABLE II. Charge density (ρ_{2D}) accumulated at the semiconductor surfaces for a series of interface systems, as a function of the potential well depth ($E_F - E_{CBM}$, in meV). The ρ_{2D} obtained considering eigenvalues and eigenfunctions as deduced from the solution of the Poisson-Schrödinger equations [theory, from Eq. (2)] is compared with the data obtained from a fitting procedure to the experimental results (Expt.).

Interface	$E_F - E_{CBM}$ (meV)	ρ_{2D} (cm^{-2}) Theor.	Expt.
InAs clean	230	3.3×10^{11}	3.9×10^{11}
Cs/InAs RT	568	2.3×10^{12}	2.3×10^{12}
Cs/InAs 200 K	600	2.6×10^{12}	2.5×10^{12}
K/InAs RT	519	2.0×10^{12}	2.1×10^{12}
Ag/InAs 80 K	524	2.0×10^{12}	1.9×10^{12}
Ag/InAs 200 K	324	7.7×10^{11}	6.8×10^{11}

the surface in order to obtain charge neutrality is comparable to the density of Ag and alkali-metal adatoms (0.01 ML corresponds to 7.7×10^{12} atoms/cm^2). On the other hand, in the case of antimony, the atomic density of the adatoms in condition of maximum band bending is much higher than the accumulated charge. The latter can be explained as a measure of defect-induced charge density localized on the dangling bonds at the Sb terrace edges, as previously suggested.

V. CONCLUSIONS

The two-dimensional electron gas, confined in the subsurface region of clean and metal-covered narrow-gap III-V(110) semiconductor surfaces, has been investigated by high-resolution and high-luminosity ultraviolet photoelectron spectroscopy. A steplike spectral density of states is measured at the bottom of the conduction band of InAs(110) and InSb(110), induced by charge accumulation and quantum confinement in the subsurface region. A number of band-bending sources is used, from alkali-metal adatoms to defect-induced states after cleavage, from Ag adsorption to Sb terrace formation. The jelliumlike 2D electron gas confined in a potential well is independent of the band-bending sources, but only dependent on the substrate band parameters and potential well shape. A self-consistent solution of the Poisson and Schrödinger equations is calculated, obtaining the eigenvalues and the eigenfunctions of the discrete energy levels, the potential well profile in excellent agreement with the whole set of photoemission results. The accumulated charge density (ranging between 3×10^{11} and 2×10^{12} charges/cm^2) can be related to the density of ''defects'' present at the semiconductor surfaces and it is comparable with experimental results obtained by means of electron scattering from free-carrier-induced plasmon modes.

[1] T. Ando, A. B. Fowler, and F. Stern, Rev. Mod. Phys. **54**, 437 (1982), and references therein.

[2] J. R. Schrieffer, in *Semiconductor Surface Physics*, edited by R. H. Kingston (University of Pennsylvania Press, Philadelphia, 1957), pp. 55–69.

[3] D. C. Tsui, Phys. Rev. Lett. **24**, 303 (1970).

[4] Y. Chen, J. C. Hermanson, and G. J. Lapeyre, Phys. Rev. B **39**, 12 682 (1989).

[5] M. G. Betti, R. Biagi, U. del Pennino, and C. Mariani, Europhys. Lett. **32**, 235 (1995).

[6] M. Noguchi, K. Hirakawa, and T. Ikoma, Phys. Rev. Lett. **66**, 2243 (1991).

[7] S. Kawaji and H. C. Gatos, Surf. Sci. **7**, 215 (1967).

[8] A. Many, I. Wagner, A. Rosenthal, J. I. Gersten, and Y. Goldstein, Phys. Rev. Lett. **46**, 1648 (1981); Y. Goldstein, A. Many, I. Wagner, and J. Gersten, Surf. Sci. **98**, 599 (1980).

[9] L. Ö. Olsson, C. B. M. Andersson, M. C. Häkansson, J. Kanski, L. Ilver, and U. O. Karlsson, Phys. Rev. Lett. **76**, 3626 (1996).

[10] V. Yu Aristov, G. Le Lay, P. Soukiassian, K. Hricovini, J. E. Bonnet, J. Osvald, and O. Olsson, J. Vac. Sci. Technol. B **12**, 2709 (1994).

[11] V. Yu. Aristov, G. Le Lay, M. Grehk, V. M. Zhilin, A. Taleb-Ibrahimi, G. Indlekofer, and P. Soukiassian, Surf. Rev. Lett. **2**, 723 (1995); V. Yu. Aristov, M. Grehk, V. M. Zhilin, A. Taleb-Ibrahimi, G. Indlekofer, Z. Hurych, G. Le Lay, and P. Soukiassian, Appl. Surf. Sci. **104**, 73 (1996).

[12] M. G. Betti, V. Corradini, V. De Renzi, C. Mariani, P. Casarini, and A. Abramo, Solid State Commun. **110**, 661 (1999).

[13] V. Yu Aristov, M. Bertolo, P. Althainz, and K. Jacobi, Surf. Sci. **281**, 74 (1993).

[14] S. Modesti, A. Falasca, M. Polentarutti, Maria Grazia Betti, V. De Renzi, and Carlo Mariani, Surf. Sci. **447**, 133 (2000).

[15] Y. Enta, T. Kinoshita, S. Suzuki, and S. Kono, Phys. Rev. B **36**, 9801 (1987); **39**, 1125 (1989).

[16] Y. C. Chao, L. S. O. Johansson, C. J. Karlsson, E. Landemark, and R. I. G. Uhrenberg, Phys. Rev. B **52**, 2579 (1995).

[17] C. Mailhiot, C. B. Duke, and D. J. Chadi, Phys. Rev. B **31**, 2213 (1985).

[18] H. Carstensen, R. Claessen, R. Manzke, and M. Skibowski, Phys. Rev. B **41**, 9880 (1990).

[19] Maria Grazia Betti, R. Biagi, U. del Pennino, M. Pedio, and Carlo Mariani, Phys. Rev. B **53**, 13 605 (1996); M. G. Betti, R. Biagi, U. del Pennino, and C. Mariani, Europhys. Lett. **32**, 235 (1995).

[20] J. Tersoff, Phys. Rev. B **32**, 6968 (1985).

[21] W. Mönch, Europhys. Lett. **7**, 275 (1988).

[22] J. Carelli and A. Kahn, Surf. Sci. **116**, 380 (1982).

[23] P. Skeath, I. Lindau, C. Y. Su, and W. E. Spicer, J. Vac. Sci. Technol. **19**, 556 (1981).

[24] L. J. Whitman, J. A. Stroscio, R. A. Dragoset, and R. J. Celotta, Phys. Rev. B **44**, 5951 (1991).

[25] R. M. Feenstra, Appl. Surf. Sci. **56−58**, 104 (1992), and references therein.

[26] C. Weisbuch and B. Vinter, *Quantum Semiconductor Structures* (Academic Press, London, 1991).

[27] The excitation lifetime is longer when the quasiparticle energy is close to the Fermi energy, i.e., $\tau = 1/(E-E_F)^{\alpha} = \hbar\Gamma^{-1}$, where $\alpha = 2$ is the 3D case. From our fitting procedure we deduce an α value of about 1.4.